CrossMark

SVCT2 Is Expressed by Cerebellar Precursor Cells, Which Differentiate into Neurons in Response to Ascorbic Acid

Karina Oyarce[1] · Carmen Silva-Alvarez[1] · Luciano Ferrada[1] · Fernando Martínez[1] ·
Katterine Salazar[1] · Francisco Nualart[1]

Abstract Ascorbic acid (AA) is a known antioxidant that participates in a wide range of processes, including stem cell differentiation. It enters the cell through the sodium-ascorbate co-transporter SVCT2, which is mainly expressed by neurons in the adult brain. Here, we have characterized SVCT2 expression in the postnatal cerebellum in situ, a model used for studying neurogenesis, and have identified its expression in granular precursor cells and mature neurons. We have also detected SVCT2 expression in the cerebellar cell line C17.2 and in postnatal cerebellum-derived neurospheres in vitro and have identified a tight relationship between SVCT2 expression and that of the stem cell-like marker nestin. AA supplementation potentiates the neuronal phenotype in cerebellar neural stem cells by increasing the expression of the neuronal marker β III tubulin. Stable over-expression of SVCT2 in C17.2 cells enhances β III tubulin expression, but it also increases cell death, suggesting that AA transporter levels must be finely tuned during neural stem cell differentiation.

Keywords Ascorbic acid (AA) · Stem cell differentiation · SVCT2 · Cerebellum · Neurogenesis · Neural stem cells

Introduction

Ascorbic acid (AA) is an essential micronutrient involved in a wide range of functions that are crucial for normal body functioning [1–4]. It is highly concentrated in the brain, particularly in the neuronal compartment, where it has been postulated to have a protective role against oxidative stress [4]. During embryonic neurogenesis, AA reaches its highest concentrations [5, 6]. Moreover, some studies have shown that AA treatment of cortical and midbrain neural precursor cells in vitro increases the expression of glial and neuronal markers [7, 8], suggesting that it could play a role in regulating neural stem cell differentiation. Recently, insight into the mechanism behind AA-mediated differentiation has been revealed, indicating that AA enhances the dopaminergic neuron phenotype of midbrain progenitors through epigenetic control [9].

In the adult brain, AA enters cells through the sodium-ascorbate transporter SVCT2, which has been detected at the choroid plexus [10, 11]; in cortical, hippocampal, and cerebellar neurons [12–14]; Schwann cells [15]; tanycytes [16]; and neural precursors from the subventricular zone [17]. In addition, we have recently described SVCT2 localization in embryonic neural stem cell radial glia (RG), specifically at the ventricular edge of the RG body, during the neurogenic phase of cortical development [18], highlighting a role for SVCT2 and AA incorporation during neurogenesis. However, further studies examining SVCT2 expression and function during the early stages of development are necessary to understand a possible role for AA during differentiation.

The cerebellar structure is a suitable model for studying neural differentiation because its cell types and migration pathways during embryonic and postnatal development have been well characterized. The presence of SVCT2 has been primarily described in the adult cerebellum [19], specifically in Purkinje neurons [17]. Our group has previously identified SVCT2 expression in the radial glial cells of the cerebellar anlage during embryonic development [12]; however, there are no detailed studies of SVCT2 expression during the early postnatal stages.

✉ Francisco Nualart
frnualart@udec.cl

[1] Centro de Microscopía Avanzada CMA-BIOBIO, Departamento de Biología Celular, Laboratorio de Neurobiología y Células Madres, Facultad de Ciencias Biológicas, Universidad de Concepción, Concepción, Chile

In the present study, we describe the spatial and temporal distribution of SVCT2 during cerebellar postnatal development, demonstrating that it is first expressed by granular precursor cells and later in mature Purkinje neurons and other small neurons in the molecular layer. We have also studied the expression, localization, and functionality of the SVCT2 transporter in cerebellar-derived neural progenitors and the effect of AA treatment on their differentiation. We have found a correlation between SVCT2 and nestin expression, demonstrating the presence of the transporter in cerebellar neural stem-like cells. Furthermore, AA treatment increased the number of cells positive for the neuronal marker β III tubulin, suggesting that it promotes the neuronal phenotype. However, when we tried to potentiate this phenomenon by stably increasing SVCT2 expression, we detected an increase in cell death, suggesting that SVCT2 expression must be tightly regulated during differentiation.

Materials and Methods

Animals Mice at 1–90 days of postnatal development (P1–P90) were used for tissue analysis and to obtain primary cerebellar cultures. The animals were maintained in a 12-h light/dark cycle with food and water ad libitum. The handling of the animals was performed in agreement with the "Manual de Normas de Bioseguridad" (Comisión Nacional de Ciencia y Tecnología (CONICYT)) and the procedures described in the publication entitled "Guide for the Care and Use of Laboratory Animals" (National Academy of Science, 2011; http://grants.nih.gov/grants/olaw/Guide-for-the-care-and-use-of-laboratory-animals.pdf).

Immunohistochemistry and Spectral Confocal Microscopy Mice from P5 to P90 were anesthetized, and 4% paraformaldehyde (PFA) was delivered by cardiac perfusion, after which the mouse brains were removed. Midsagittal brain slices were postfixed in the same fixative for 24–48 h at 4 °C. P1 mice were decapitated, and their brains were fixed by immersion in 4% PFA at 4 °C for 24 h. The tissues were embedded in 2% agarose molds for vibratome sectioning. Sections of 50 μm were incubated overnight at 4 °C with the following antibodies diluted in Tris-phosphate buffer and 4% bovine serum albumin: anti-SVCT2 H70 (1:50, Santa Cruz Biotechnology, CA, USA), anti-vimentin (1:200, EMD Millipore, Darmstadt, Germany), anti-β III tubulin (1:500, clone Tuj1, Promega Corporation, Madison, WI, USA), and anti-PCNA (1:200, Agilent Technologies, Dako, Glostrup, Denmark). The samples were then incubated with the appropriate secondary antibody conjugated to different fluorophores, including Alexa 488-conjugated goat anti-rabbit, Cy^5-conjugated donkey anti-chicken, and Cy^3-conjugated donkey anti-mouse (1:200, Jackson ImmunoResearch, West Grove, PA, USA). TO-PRO-3 or Hoechst 33,342 (1:1000, Thermo Fisher Scientific Inc., MA, USA) was used for nuclear staining. The sections were mounted using fluorescence mounting medium (Agilent Technologies). The tissue samples and cell cultures were analyzed by confocal microscopy (LSM700, Zeiss) or spectral confocal microscopy (LSM780 NLO, Zeiss). Images were acquired with ZEN 2011 software (Zeiss) with a size of 1024 × 1024 × 16 bits. The fluorescence intensity parameters for each channel, such as laser power and digital gain, were set using samples without primary antibody as negative controls for background-level normalization. For tissue samples and neurospheres, images were taken as a z-stack for maximum intensity projection (MIP) images and 3D reconstructions. For the analysis of thick cerebellar tissue from mice at P90, an automatized segmented scanning was performed in the x, y, and z planes, with a ×40 objective, using the tile scanning mode.

Cell Line and Cerebellar Primary Culture The C17.2 cell line (Sigma-Aldrich, St. Louis, MO, USA) was grown in Dulbecco's modified Eagle's medium (Gibco Thermo Fisher Scientific Inc., MA, USA) supplemented with 10% fetal bovine serum (HyClone Laboratories, Logan, UT, USA), 5% horse serum (Gibco), penicillin, and 1% glutamine. Primary cultures were obtained from 4-day-old murine cerebellar tissues. The tissue was dissected and mechanically disaggregated in NSC proliferation medium (Stem Cell Technologies, Vancouver, BC, Canada) supplemented with epidermal growth factor (EGF; 20 ng/mL), fibroblast growth factor (FGF; 10 ng/mL), and heparin (10 ng/mL) (Stem Cell Technologies). The supernatant was collected and centrifuged at 800 rpm for 5 min. The cell viability was determined using the trypan blue exclusion method. The cell pellets were resuspended in fresh NSC proliferation medium, and the cellular suspension was seeded in Corning Ultra Low Attachment cell culture flasks (Sigma-Aldrich) at approximately 60,000 cells/cm^2 to allow for neurosphere formation. After 4 days in vitro (DIV), the neurospheres were collected and centrifuged at 400 rpm for 5 min. The pellet was resuspended in fresh NSC proliferation medium with or without growth factors and allowed to adhere to poly-L-lysine-coated dishes (0.5 mg/ml poly-L-lysine; Sigma-Aldrich). For differentiation assays, AA (Sigma-Aldrich) was added periodically to cultures at a final concentration of 200 or 400 μM. The culture medium was changed every 2 or 3 days. All cultures were incubated in 5% CO_2 in a humidified chamber at 37 °C.

Immunocytochemistry NSCs were grown on poly-L-lysine-coated coverslips (0.5 mg/ml poly-L-lysine; Sigma-Aldrich),

whereas C17.2 cells were seeded on uncoated coverslips. The cells were fixed with methanol for 10 min or 4% PFA in PBS for 30 min at room temperature and washed with Tris-phosphate buffer. The cells were incubated overnight at room temperature with the following antibodies diluted in Tris-phosphate buffer with 1% bovine serum albumin: anti-nestin (1:100, BD Biosciences, San Jose, CA, USA), anti-GFAP (1:100, Agilent Technologies, Dako, Glostrup, Denmark), anti-β III tubulin (1:5000), and anti-SVCT2 (1:25, Santa Cruz Biotechnology, CA, USA). The cells were incubated with Cy2-conjugated affinity-purified donkey anti-goat IgG, donkey anti-rabbit IgG, or donkey anti-mouse IgG (1:200; Jackson Immuno-Research, PA, USA) at room temperature for 2 h. TO-PRO-3 or Hoechst 33,342 (1:1000) was used for nuclear staining. The fluorescence intensity parameters for each channel, such as laser power and digital gain, were set using samples without primary antibody as negative controls for background-level normalization.

In Situ Hybridization In situ hybridization was performed on P15 mouse cerebellar sections mounted on poly-L-lysine-coated glass slides, using a 0.6-kb digoxigenin-labeled riboprobe for SVCT2 as described by García et al. [16].

RT-PCR Total RNA was isolated using TRIzol (Invitrogen, Rockville, MD, USA). For the reverse transcription reaction, 2 μg of RNA was incubated with DNase I (New England Biolabs, Ipswich, MA, USA) for 30 min at 37 °C and with 2.5 mM EDTA at 65 °C for 10 min. The reaction proceeded in a 20-μL total reaction volume containing 10 mM Tris-HCl, 50 mM KCl, 5 mM MgCl$_2$, 20 U RNase inhibitor, 1 mM dNTPs, 2.5 μM oligo d(T) primers, and 50 u of MuLV reverse transcriptase (New England Biolabs) for 5 min at 70 °C followed by 5 min at 37 °C, 1 h at 42 °C, and 10 min at 70 °C. Parallel reactions were performed in the absence of reverse transcriptase to control for the presence of contaminant DNA. For amplification, 1 μL of cDNA was added to a total reaction volume of 12.5 μL containing 20 mM Tris-HCl, 50 mM KCl, 1.6 mM MgCl$_2$, 0.4 mM dNTPs, 0.04 u of *Taq* DNA polymerase (Invitrogen), and 0.4-mM primers. The mix was incubated for 5 min at 95 °C followed by 35 cycles of 30 s at 95 °C, 30 s at the appropriate annealing temperature (50–60 °C), and 30 s at 72 °C with a final extension at 72 °C for 5 min. The PCR products were separated by 1% agarose gel electrophoresis and visualized by ethidium bromide staining. The following primers were used: cyclophilin, f5′-ATAATGGCACTGGTGGCAAGTC-3′ and r5′-ATTCCTGGACCCAAAACGCTCC-3′; β-actin, f5′-GCTGCTCGTCGACAACGGCTC-3′ and r5′-CAAA CATGATCTGGGTCATCT TCTC-3′; SVCT2 (qPCR), f5′-TGTTTCAGGCCAGTGCTTTT-3′ and r5′-TGTA TGCCGTCCATCCTTTC-3′; SVCT2 (full length), f5′-ATGA

TGGGTATCGGCAAGAAC-3′ and r5′-CTATACTGTGGCCT GGGAATCTTT-3′; and SVCT2 (rat), f5′-GCTC ATCGGGACCATTTTCT-3′ and r5′-CATAGCAGTGGTGA GAAGGA-3′.

Western Blot Analysis Total proteins extracted from C17.2 cells at 3 or 9 DIV were obtained by detaching the cells from the culture plates with trypsin/EDTA followed by centrifugation at 1000 rpm for 5 min. The pellet was homogenized with a protease inhibitor solution (Roche Applied Science, IN, USA), sonicated at 60 Hz, and centrifuged at 4000 rpm for 10 min. The proteins in the supernatant were quantified using the Bradford method. For immunoblotting, 50 or 100 μg of total protein was loaded onto a 5–15% gradient polyacrylamide gel and separated by electrophoresis in the presence of sodium dodecyl sulfate; transferred to PVDF membranes (0.45-μm pore; Amersham Pharmacia Biotech, Piscataway, NJ, USA); and probed with anti-SVCT2 (1:200, Santa Cruz Biotechnology), anti-nestin (1:200, BD Biosciences, San Jose, CA, USA), anti-β III tubulin (1:5000, clone Tuj1), or anti-actin (1:1000, Santa Cruz Biotechnology) antibodies. The membranes were then incubated with the secondary antibodies, including HRP-conjugated donkey anti-goat IgG, donkey anti-rabbit IgG, or donkey anti-mouse IgG (1:5000; Jackson Immuno-Research, PA, USA), at room temperature. The reaction was developed using the Western Lighting® Plus-ECL enhanced chemiluminescence substrate (Perkin Elmer, Waltham, MA, USA).

AA Uptake Assays C17.2 cells were seeded in 6-well plates at a normal density (5000 cells/cm^2). After 3 or 9 DIV, the cells were incubated in a buffer containing 15 mM HEPES, 135 mM NaCl, 5 mM KCl, 1.8 mM CaCl$_2$, and 0.8 mM MgCl$_2$ at room temperature for 10 min or a buffer in which NaCl was replaced by choline chloride, when indicated. The incubation buffer was replaced with ^{14}C–AA (DuPont NEN, Boston, MA, USA; specific activity 8.2 mCi/mmol) diluted in the same buffer at a final concentration of 50 or 100 μM.

Cloning of SVCT2 and Lentiviral Particle Production for Over-Expression The complete coding sequence for SVCT2 was obtained by RT-PCR from E18 murine brain extracts and cloned into the lentiviral vector pLB, a gift from Stephan Kissler (Addgene plasmid #11619), in frame at the N-terminal region of the *GFP* reporter gene. Vesicular stomatitis virus-pseudotyped lentivirus was produced in HEK 293 T cells by calcium phosphate transient co-transfection of the transfer vectors pLB or pLB-SVCT2, the packaging constructs pR5V-Rev and pCMVdR8.74,

and the vesicular stomatitis virus envelope-expressing construct pMD2.VSVG, as described in Salazar et al. [20]. The supernatants were collected after 30 h and filtered for cell line transduction.

Lentiviral Transduction of the C17.2 Cell Line for SVCT2 Over-Expression and GFP-Positive Cell Enrichment Through Fluorescence-Activated Cell Sorting C17.2 cells were seeded at a normal density (5000 cells/cm^2) 48 h prior to transduction. The cells were incubated in a mixture of lentiviral supernatant and fresh culture medium (1:1) in the presence of 7 μg/mL of polybrene (Sigma-Aldrich) for 4–6 h, after which the culture medium was changed. After 48 h, the transduced cells were dissociated with trypsin/EDTA, pelleted, and suspended in PBS at a density of 10^6 cells/mL. The cell suspension underwent fluorescence-activated cell sorting (FACS) enrichment using a BD FACSAria III cell sorter. Non-transduced cells were used as a negative control for the sorting. Both the GFP- and GFP-SVCT2-sorted fractions were seeded again for analysis and expansion.

Cell Viability Analysis with FACS The effect of SVCT2 over-expression on C17.2 cell viability was evaluated at 2, 4, and 8 days after FACS enrichment. The cells were dissociated with trypsin/EDTA, pelleted, and suspended in PBS at a density of 10^6 cells/mL. Before the analysis, each culture was incubated with a propidium iodide (PI) solution (50 μg/mL)

for 30 min at 37 °C in the dark. As a positive control for PI incorporation, cell death was induced in non-transduced cells exposed to thermic shock at 60 °C for 5 min. Using the BD FACSAria III cell sorter, the PI-positive cells were counted in each cell suspension by flow cytometry analysis in the phycoerythrin (PE) channel, and GFP fluorescence was evaluated in the fluorescein isothiocyanate (FITC) channel.

Results

SVCT2 Expression During Postnatal Cerebellar Development

We first analyzed SVCT2 messenger RNA (mRNA) levels by real-time RT-PCR at 1, 7, 21, and 60 days after birth. We were able to detect SVCT2 mRNA levels at every time point examined, observing a large increase in its levels during the third postnatal week, followed by a decrease at the more adult stage of P60 (Fig. 1a). In situ hybridization for SVCT2 on P15 cerebellar sections showed localization in the somas of Purkinje neurons and not in Bergmann glial processes (Fig. 1b, d), as corroborated by GFAP immunodetection in the same section (Fig. 1c, e).

The SVCT2 distribution at the protein level was analyzed using quadruple immunofluorescence staining with spectral confocal microscopy to associate SVCT2 expression with markers of different cell types. At P1, the AA transporter
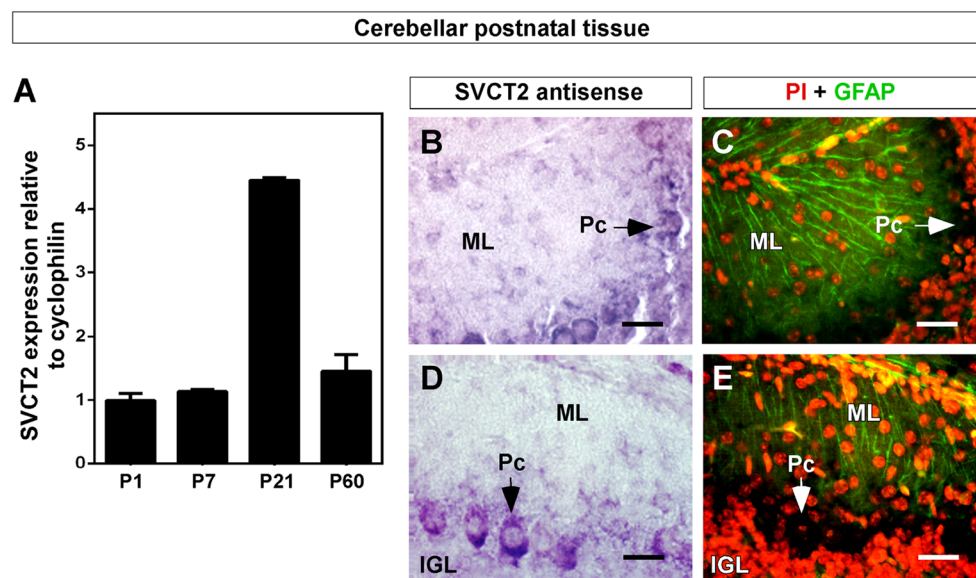
Fig. 1 SVCT2 expression in postnatal cerebellar tissue. **a** Total RNA was isolated from cerebellar tissue at different time points of postnatal development, and real-time PCR was performed to measure the changes in SVCT2 mRNA expression levels compared with cyclophilin. **b, d** In situ hybridization for SVCT2 on cerebellar sections at postnatal day 15 using an anti-sense probe for SVCT2. **c, e** Immunofluorescence analysis for GFAP (green) and propidium iodide (red) in the same cerebellar section. SVCT2 immunoreactivity is detected in Purkinje neurons (purple staining, arrow) and not associated with Bergmann glia. ML molecular layer, IGL internal granular layer, Pc Purkinje cells. Scale bar in **b–e**, 20 μm

was detected in the outermost region of the cerebellar cortex, corresponding to the external granular layer (EGL) (Fig. 2b, f), a highly proliferative germinal zone, as shown with PCNA staining (Fig. 2a, e). No reactivity was seen in the white matter. The intermediate filament protein vimentin was used to detect the Bergmann fibers that run throughout the EGL (Fig. 2c, g). Double staining for SVCT2 and vimentin initially showed some degree of co-localization (Fig. 2d), but an analysis at a higher magnification showed that the vimentin-positive processes were SVCT2-negative below the EGL, illustrating that the co-localization is most likely due the close proximity between Bergman glial processes and the granular precursors in the EGL (Fig. 2h).

At P5, SVCT2 was heterogeneously distributed in the EGL, preferentially at the lobes instead of the internal fissures (Fig. 2i). However, the greatest immunoreactivity was observed in a transition zone between the granular precursors and the differentiated granular neurons (Fig. 2i, arrows), co-localizing with the neuronal marker β III tubulin (Fig. 2j, l, m). Some faint immunoreactivity was also detected for SVCT2 in the newly formed internal granular layer (IGL) (Fig. 2i).

At P15, SVCT2 was absent from the EGL but was detected in a diffuse pattern in the molecular layer (Fig. 2n), co-localizing with β III tubulin (Fig. 2o, q) and exhibiting no association with vimentin expression (Fig. 2p). The strongest reaction for the transporter was observed in the soma of Purkinje neurons and in their projections into the molecular layer, whereas minimal expression was detected in the IGL (Fig. 2n, arrows). For the first time, SVCT2 expression was observed in scattered cells present in the white matter tracts; some of which were negative for β III tubulin (Fig. 2r, asterisks).

The fully mature, adult cerebellar cortex is a complex structure in which the dendrites of Purkinje neurons, Bergman glial fibers, and other small neurons located in the molecular layer establish different connections. To gain a more comprehensive understanding of this organization, we examined thick P90

Fig. 2 Characterization of SVCT2 expression in murine cerebellar tissue during early postnatal development. Cerebellar sections at postnatal day 1 were stained for vimentin (*green*) and PCNA (*red*) (**a**, **e**) or triple stained for SVCT2 (*green*), vimentin (*red*), and the nuclear dye Hoechst (*blue*) (**b–d**, **f–h**). Cerebellar sections at postnatal day 5 (**i–m**) and postnatal day 15 (**n–r**) were quadruple stained for SVCT2 (*green*), β III tubulin (*red*), vimentin (*gray*), and Hoechst (*blue*). SVCT2 expression is detected first in granular precursor cells from the EGL, later in a transition zone between the EGL and IGL, and finally in Purkinje neurons. *Scale bars* 100 μm (**b–d**, **i–l**, **n–q**) and 50 μm (**a**, **e–h**). *EGL* external granular layer, *IGL* internal granular layer, *ML* molecular layer, *Pc* Purkinje cells, *WM* cerebellar white matter
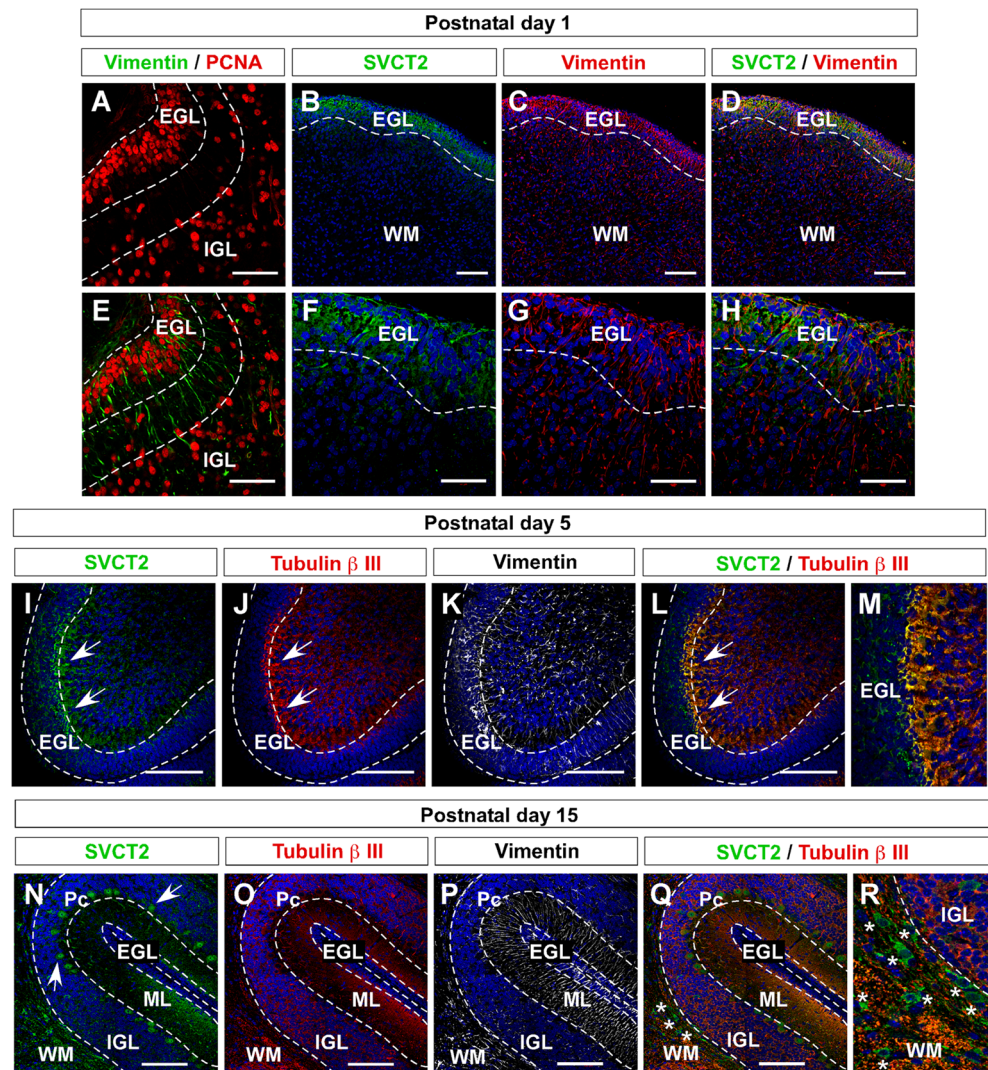
cerebellar sections using the tile scanning mode and a z-stack projection. Our results show how the dendritic processes of Purkinje neurons are projected at different depths into the molecular layer, becoming thinner and more numerous when they reach the outermost region (Fig. 3a). In contrast, vimentin-positive Bergmann fibers appear to be perfectly aligned and oriented in the same direction as the Purkinje processes (Fig. 3b); however, an analysis of higher-magnification images showed that some glial fibers exhibited short branches as well (Fig. 3d).

When SVCT2 expression was analyzed, we detected its presence only in the neuronal compartment, observing a strong signal in the soma and primary branches of Purkinje neurons (Fig. 3e, i, arrows). SVCT2 expression is also detected in some small neurons in the upper part of the molecular layer (Fig. 3i, asterisks), whereas very low immunoreactivity is observed in the IGL. No reactivity for SVCT2 was detected in the white matter tracks. Double staining for SVCT2 (green) and vimentin (white) showed no association between these two markers (Fig. 3j), whereas SVCT2 and β III tubulin exhibited a tight co-localization (Fig. 3k, l).

SVCT2 Expression in Cerebellar Precursor Cells

Once the cerebellar SVCT2 expression was defined, we characterized its functionality in cerebellar neural stem cell cultures. We first used the multipotent murine cell line C17.2, derived from 4-day-old mice cerebellum tissue [21], which expresses the neural stem cell marker nestin (Fig. 4a, c). At the beginning of the culture, every cell was positive for nestin, and only a few were positive for β III tubulin expression (Fig. 4a, b). However, the cell line exhibited a spontaneous increase in the number of β III tubulin-positive cells when maintained in culture (Fig. 4c, d), suggesting that under standard culture conditions, this model has some level of neuronal commitment.

SVCT2 expression was analyzed in C17.2 cells at 3 and 9 DIV by RT-PCR, immunocytochemistry, and Western blot analyses.

We were able to detect SVCT2 mRNA and protein expression (Fig. 4e–h), finding low levels of expression at 3 DIV and an increase in SVCT2 protein at 9 DIV (Fig. 4e, f, h). Although the immunocytochemical analysis showed that SVCT2 was localized predominantly in the intracellular compartment (Fig. 4e, f), functional assays measuring radioactive AA uptake confirmed that C17.2 cells incorporated AA in a sodium-

Fig. 3 SVCT2 expression and adult cerebellar cortex architecture. **a–d** Deep imaging with color-coded projection of β III tubulin (**a**) and vimentin (**b**) staining. Higher-magnification images are shown in **c**, **d**. *Blue to red shades* on the color bar represent the deeper and more superficial layers, respectively. **e–g**, **i–k** Maximum intensity projection of adult mouse cerebellar sections stained with SVCT2 (*green*), β III tubulin (*red*), vimentin (*gray*), and the nuclear dye Hoechst (*blue*). *Z-stack thickness 19 μm. **h**, **l** Higher-magnification images of **g**, **k**, respectively. *Scale bars* 200 μm (**e–g**) and 100 μm (**i–k**). *ML* molecular layer, *IGL* internal granular layer, *Pc* Purkinje cells
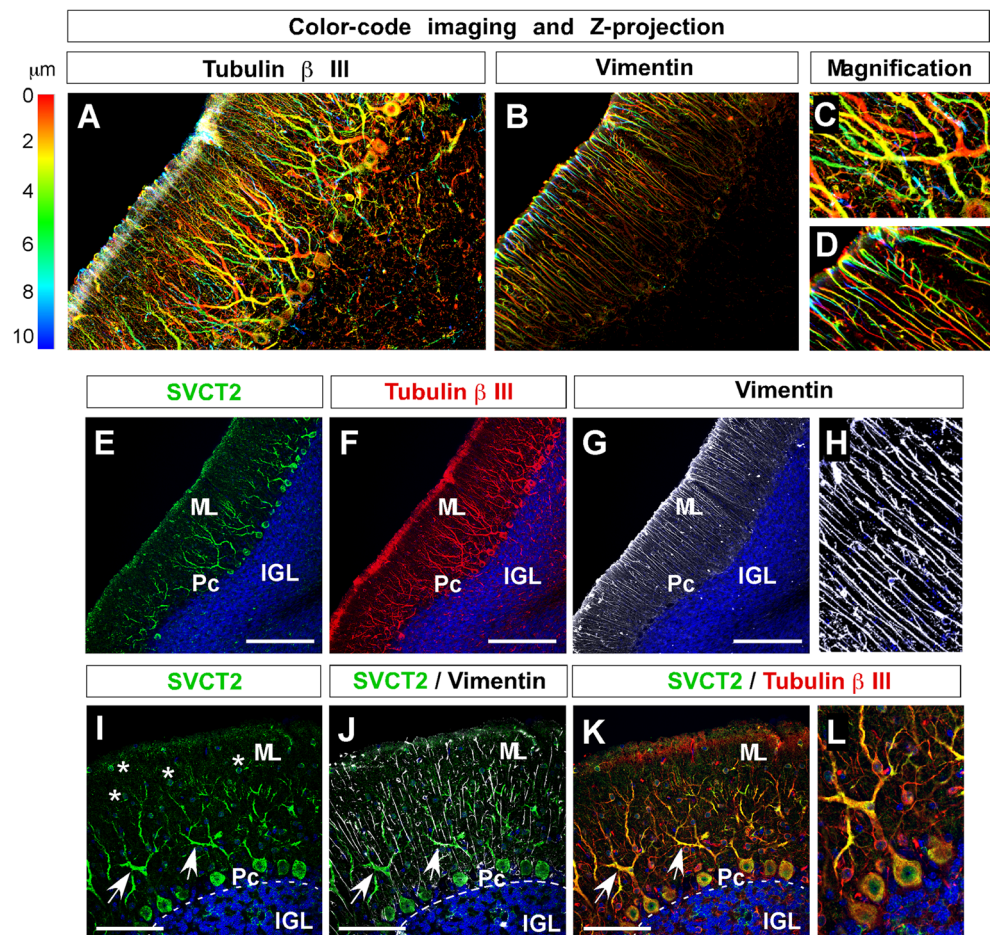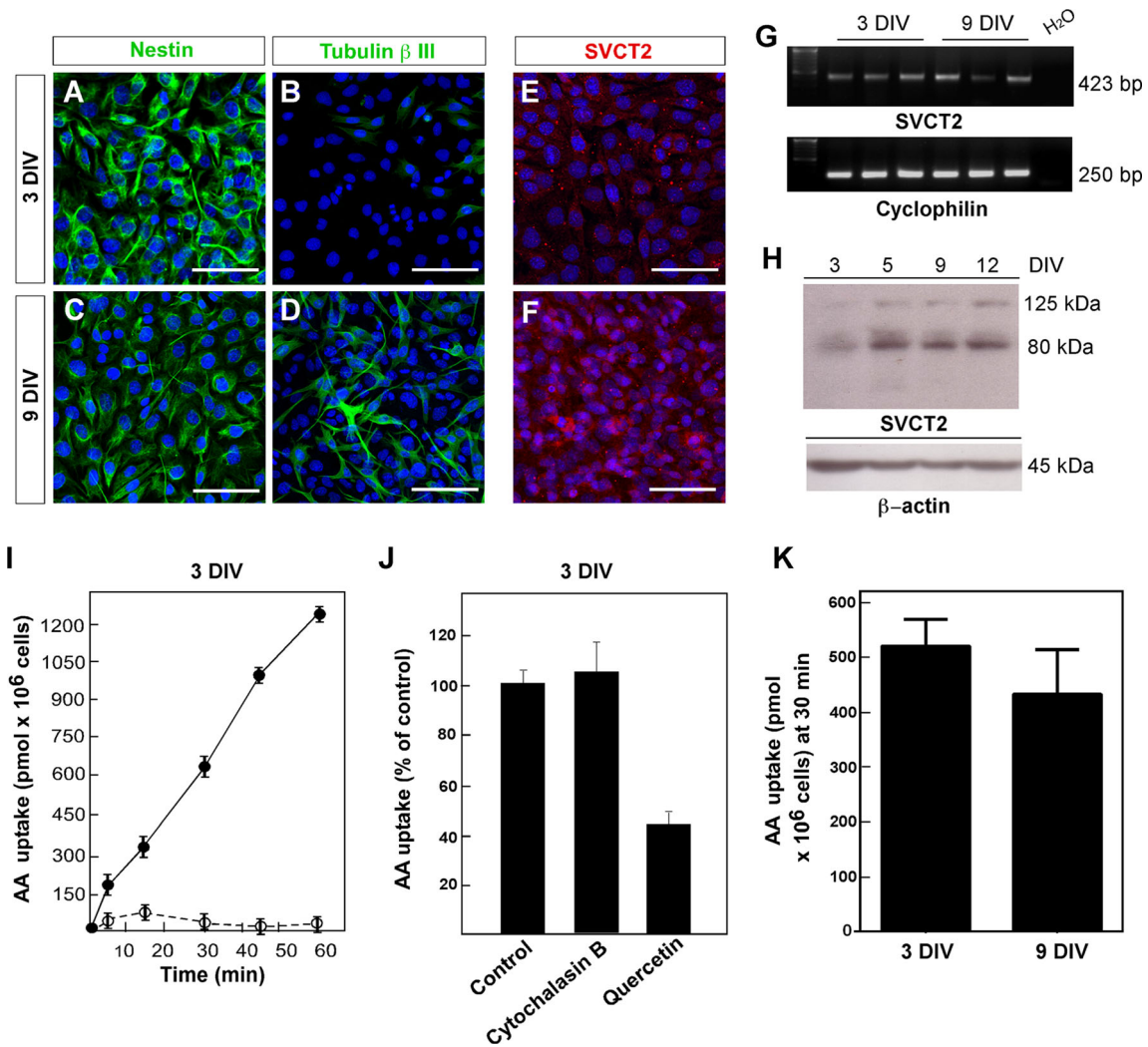
Fig. 4 The multipotent cerebellar cell line C17.2 expresses SVCT2. **a–d** Immunocytochemical characterization of the multipotent cerebellar cell line C17.2 at 3 and 9 days in vitro (DIV) for nestin, β III tubulin, and the nuclear dye Topro-3 (*blue*). The C17.2 cell line shows the spontaneous neuronal differentiation. **e, f** C17.2 cells after 3 and 9 DIV stained with SVCT2 (*red*) and TO-PRO-3 (*blue*). **g** Total RNA was isolated from C17.2 cell cultures at 3 and 9 DIV, and the mRNA expression of SVCT2 and cyclophilin was evaluated by RT-PCR. **h** SVCT2 protein expression was also detected by Western blot analysis, showing a predicted major band of 80 kDa at 3, 5, 9, and 12 DIV that increases over time when compared to β-actin expression. **i–k** AA uptake measurements in C17.2 cells using -L-(C^{14})- AA at 37 °C in the presence of 50 mM AA and 0.1 mM DTT. **i** Progress curve for AA uptake at 3 DIV. *White circles* correspond to AA uptake in the absence of sodium ions. **j** The 30-min AA uptake at 3 DIV in the presence of the GLUT inhibitor cytochalasin B and the SVCT2 inhibitor quercetin, showing that AA uptake is mediated by SVCT2. **k** AA uptake at 3 and 9 DIV after 30 min, showing no significant differences. *Scale bars* **a–f** 100 μm

dependent manner, exhibiting a 95% inhibition in uptake when sodium ions were removed from the media (Fig. 4i). AA transport was also inhibited by the flavonoid quercetin, as reported in a previous study by Caprile et al. [12]. However, it was not affected by cytochalasin B, a known inhibitor of the uptake of the oxidized form of vitamin C (DHA) by GLUTs (Fig. 4j). Even though we have recently reported AA uptake by this cell line [18], we demonstrate in this study that these cells maintain the ability to incorporate vitamin C in a sodium-dependent manner for a longer period of time. Between 3 and 9 DIV, no significant changes in AA uptake were detected (Fig. 4k), indicating that the higher levels of SVCT2 expression observed do not translate into a functional gain.

As a second cerebellar model, we obtained primary cultures from murine P4 whole cerebellar samples, which were the same age as the origin tissue of the C17.2 cell line. To select for neural stem-like cells, neurosphere formation was induced by incubating the cell suspension in an NSC culture medium supplemented with the growth factors FGF and EGF. By RT-PCR, we detected SVCT2 expression in the cultures after 2 days of direct seeding as well as in cultures at 2 days after neurosphere formation (Fig. 5a). An immunocytochemical characterization of both cultures for nestin, GFAP, and β III tubulin expression showed an enrichment of nestin-positive cells (Fig. 5b, e), an increase in GFAP expression (Fig. 5c, f), and a reduction in β III tubulin expression (Fig. 5d, g)
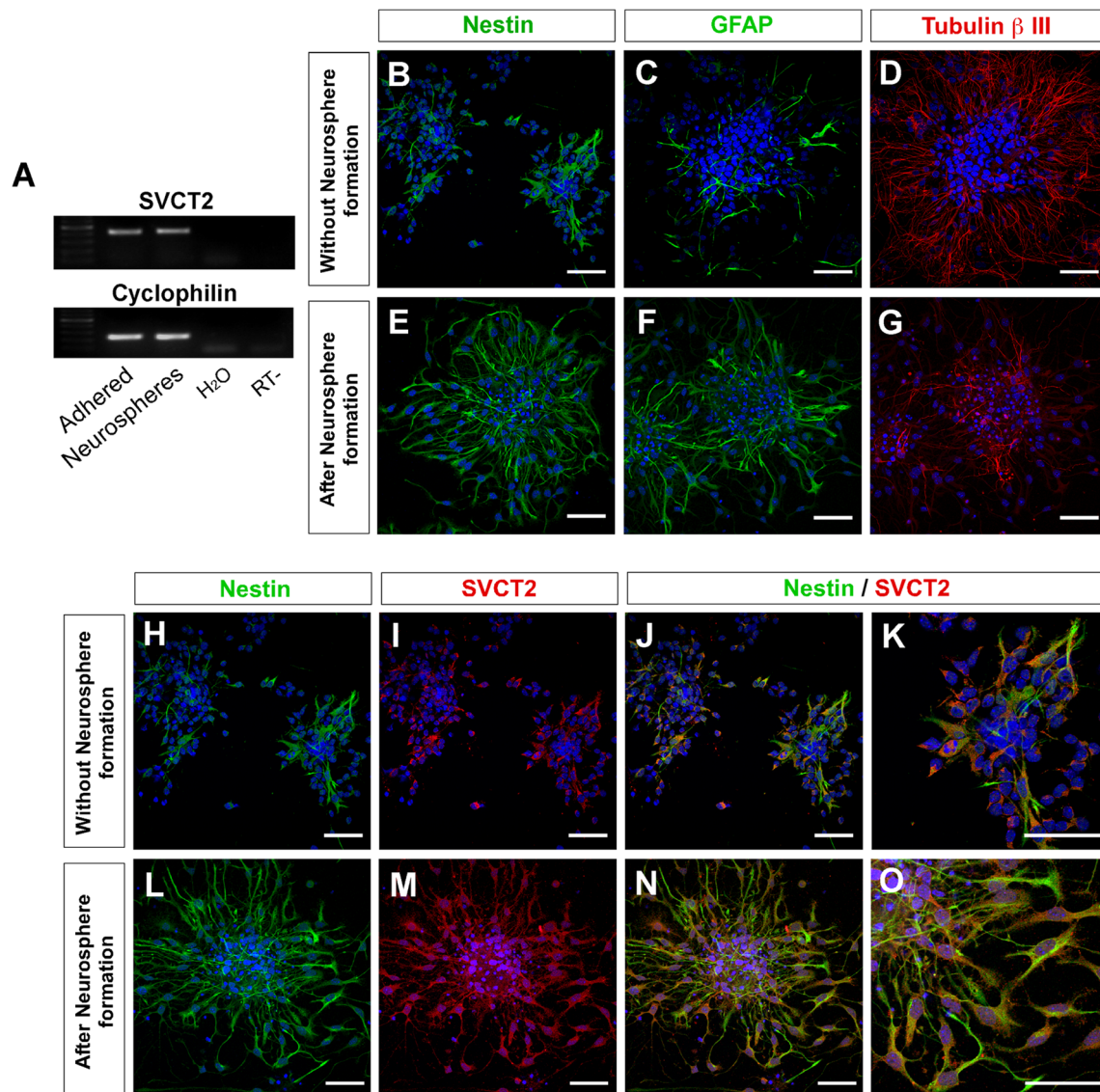
Fig. 5 Postnatal day 4 cerebellar neuronal precursors express SVCT2. **a** Total RNA was isolated from adhered cerebellar cultures at 2 days in vitro (DIV) and from 4 DIV cerebellar neurospheres grown in suspension. SVCT2 and cyclophilin mRNA levels were evaluated by RT-PCR. **b–g** Immunocytochemical staining of P4 cerebellar cultures with or without neurosphere formation for nestin (*green*), GFAP (*green*), β III tubulin (*red*), and the nuclear stain TO-PRO-3 (*blue*). Enrichment of nestin-positive cells is observed after neurosphere formation. **h–o** Immunocytochemical staining with nestin (*green*) and SVCT2 (*red*) as well as nuclear staining with TO-PRO-3 (*blue*) of adhered cerebellar cultures and 4 DIV cerebellar neurospheres adhered for 2 days. Co-localization is observed between SVCT2 and nestin. *Scale bars* 50 μm (**b–g, h–j, l–n**) and 25 μm (**k, o**)

following neurosphere formation, confirming the selection of cells that have a more undifferentiated phenotype.

The immunofluorescence analysis also showed that the neurospheres were enriched with SVCT2-positive cells (Fig. 5i, m). Compared with the C17.2 cell line, the cerebellar primary cultures exhibited a higher fluorescence intensity for SVCT2 immunoreactivity (Fig. 5m). Double staining for nestin and SVCT2 revealed co-localization in both types of cultures (Fig. 5j, k, n, o), showing a tight association between SVCT2 expression and the neural stem cell phenotype.

AA Increases the Expression of the Marker β III Tubulin in the Cerebellar Cell Line C17.2

We next evaluated the effect of AA on C17.2 cell differentiation by analyzing nestin and β III tubulin expressions after treatment with 200 or 400 μM AA for 9 DIV. In contrast to the other differentiation protocols, we did not remove bovine and horse serum during the AA treatment. Both immunocytochemistry and Western blot analyses showed that AA decreased the expression of nestin (Fig. 6a–d, m) but not the number of nestin-positive cells, which remained at approximately 95%. We also
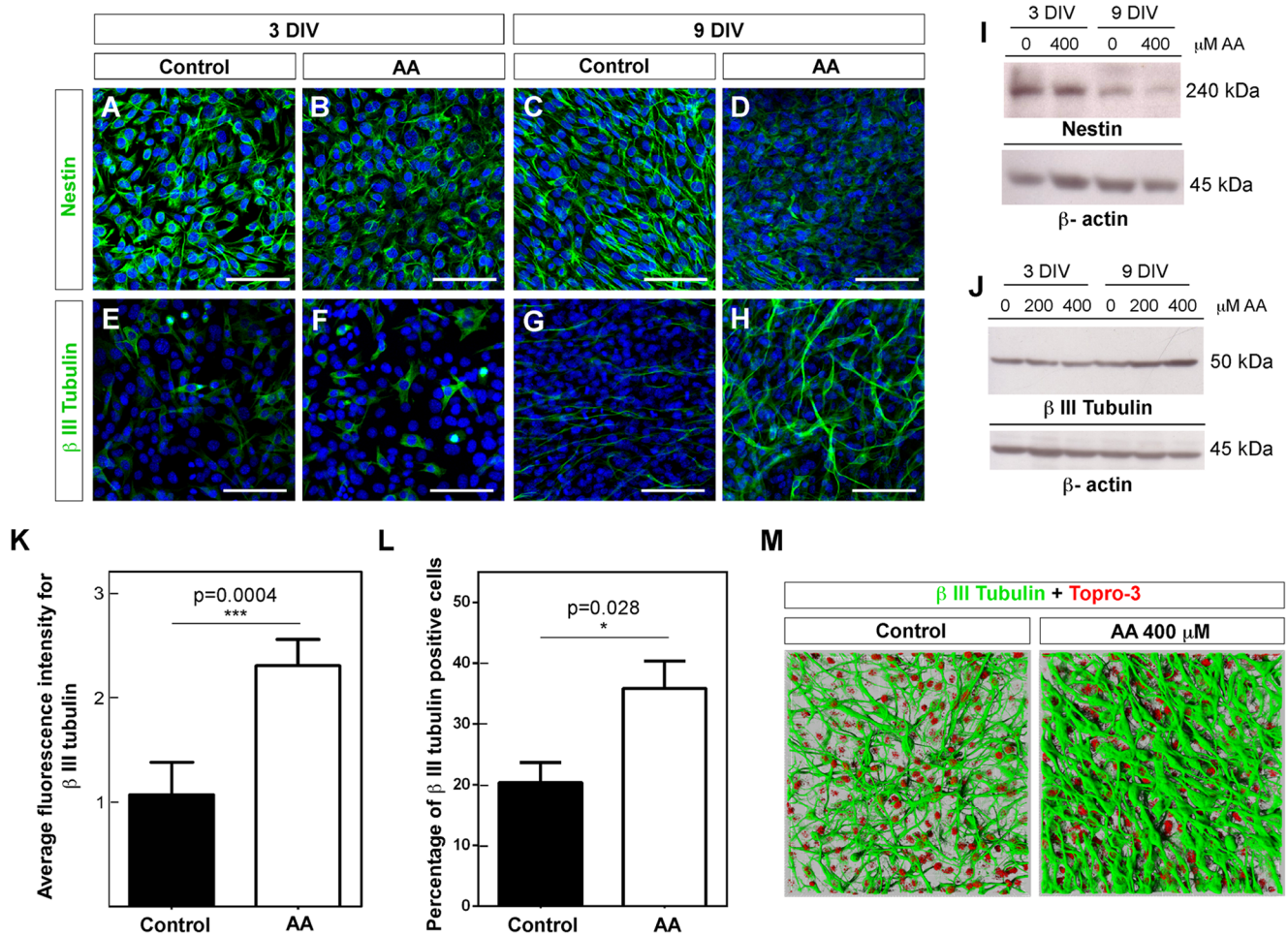
Fig. 6 AA treatment increases β III tubulin expression in C17.2 cell cultures. **a–h** Immunocytochemical staining of C17.2 cells at 3 and 9 DIV without passaging for nestin (*green*), β III tubulin (*green*), and the nuclear dye TO-PRO-3 (*blue*) following treatment with 400 μM AA. The control cells were not treated with AA. The noticeable effects of AA on culture phenotype are shown at 9 DIV, where AA reduces nestin expression and increases β III tubulin. *Scale bars* 50 μm. **i**, **j** Nestin and β III tubulin protein expressions were detected by Western blot analysis, showing a decrease in nestin expression (**i**) and an increase in β III tubulin expression (**j**) over time when compared to β-actin. **k**, **l** The tubulin β III fluorescence intensity (**k**) and the number of positive cells (**l**) were quantified in 9 DIV C17.2 cultures. An increase in both the number of β III tubulin-positive cells and their thickness is observed. The results represent the mean ± SD ($n = 9$ for each group of four independent experiments). The nonparametric statistical analysis was performed using the Mann-Whitney posttest. **$P < 0.005$, ***$P < 0.001$. **m** Representative 3D reconstruction images of the maximum projection intensity for C17.2 cells at 9 DIV treated with or without AA and stained for β III tubulin (*green*). The *red spheres* represent nuclei. Imaris (BitPlane) software was used

observed that β III tubulin expression was higher in AA-treated cultures after 9 DIV (Fig. 6g, h, n), with increases seen in both the number of positive cells (from 20.3 ± 3.4 to 35.8 ± 4.5%) and the marker immunoreactivity, which was higher by a factor of two (Fig. 6k, l). This increase in neuronal marker expression at 9 DIV could be clearly observed when different *z* planes of the cultures were used to create a 3D reconstructed image that showed thicker processes when AA was added to the cultures (Fig. 6m). The fact that changes in the expression of the differentiation markers were detected after several days of AA supplementation indicates that chronic instead of acute AA administration is required in order to see an effect on differentiation.

SVCT2 Over-Expression Increases the Neuronal Phenotype but Also Has an Effect on Cell Death

To study the relationship between SVCT2 expression and neural stem cell differentiation in more detail, we performed gain-of-function studies through lentivirus-mediated stable over-expression of SVCT2 fused with green fluorescent protein (GFP) or GFP alone in the C17.2 cell line. The transduced cells were then sorted for GFP fluorescence via FACS flow cytometry, monitoring GFP fluorescence in the FITC channel to enrich for efficiently transduced cells (Fig. 7a–f). The flow cytometry analysis showed that cultures transduced with SVCT2-expressing lentivirus had fewer positive events and lower fluorescence signal intensities when compared with
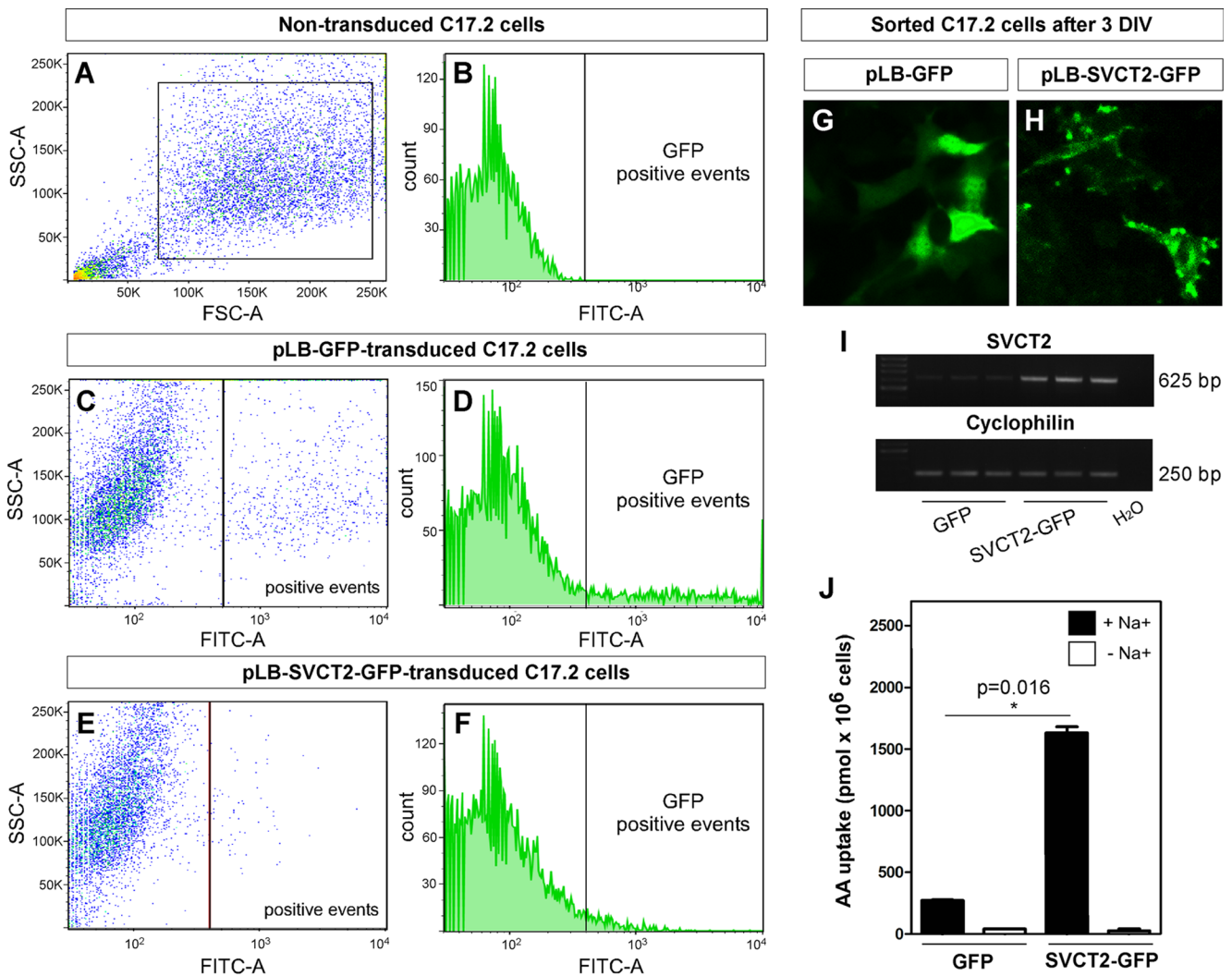
Fig. 7 SVCT2 over-expression analysis in the C17.2 cell line. **a–f** GFP and SVCT2-GFP compensations by fluorescent-activated cell sorting (FACS) of the transduced C17.2 cells using non-transduced cells as a negative control. **a** The two-dimensional plot of the forward scatter (FSC) versus side scatter (SSC) of the non-transduced cells shows the gate selection for further FACS. **b** Histogram for GFP expression detection in non-transduced cells using the FITC channel and the fluorescence parameters for defining a GFP-positive population. **c, e** Two-dimensional plot of the GFP signal using the FITC channel versus the SSC of C17.2 cells transduced with pLB-GFP (**c**) or pLB-SVCT2-GFP (**e**). **d, f** Histograms for GFP expression detection using the FITC channel of C17.2 cells transduced with empty vector (**d**) or SVCT2 (**f**). pLB-GFP-transduced cultures exhibit more GFP-positive cells with higher fluorescence intensity levels when compared with pLB-SVCT2-GFP-transduced cultures. **g, h** Epifluorescence microscopy live-cell imaging of C17.2 cells following FACS showing transgene expression and SVCT2 localization. **i** Total RNA was isolated after 3 DIV following FACS, and the mRNA expressions of SVCT2 and cyclophilin were evaluated by RT-PCR. **j** AA uptake measurements in C17.2 cells after 3 DIV following FACS using L-[^{14}C]-AA at 37 °C in the presence of 50 mM AA and 0.1 mM DTT (*white bars* correspond to AA uptake in the absence of sodium ions). A sixfold increase in AA uptake is seen when compared with cells transduced with an empty vector. The results represent the mean ± SD ($n = 6$ for each group of two independent experiments). The nonparametric statistical analysis was performed using the Mann-Whitney posttest. *$P < 0.05$

cultures transduced with the empty vector expressing GFP alone (Fig. 7c–f).

GFP-positive cells were selected for seeding and further experimental analysis. After 3 days of culture, the GFP expression was evaluated by live fluorescence microscopy, demonstrating the successful enrichment of transduced cells (Fig. 7g, h). The cell morphology was altered when SVCT2 was over-expressed, exhibiting filopodia like-structures, and SVCT2 expression was mainly distributed within the cytoplasm, with focally concentrated points presumably in membrane borders (Fig. 7h). SVCT2 over-expression was also confirmed by RT-PCR (Fig. 7i), but more importantly, the AA uptake was increased by sixfold (from 250 pmol x 10^6 cells in control cultures to 1650 pmol x 10^6 cells in SVCT2-over-expressing cultures), showing that SVCT2 over-expression translated in a functional gain (Fig. 7j).

At 8 DIV, the transduced cells were analyzed for β III tubulin expression by immunocytochemistry (Fig. 8a–f). Our
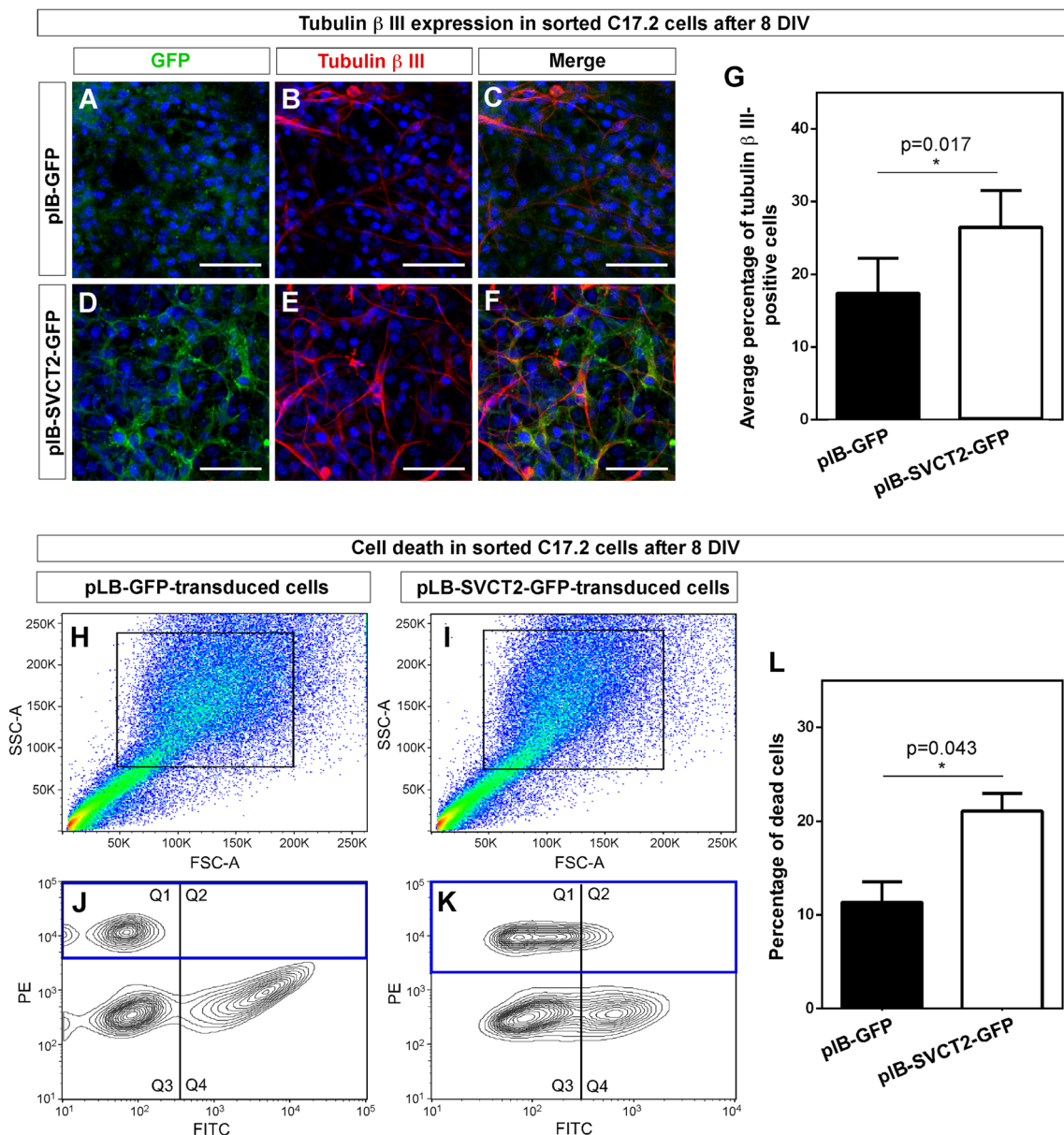
Fig. 8 SVCT2 over-expression in the C17.2 cell line increases cell death. **a–f** Immunostaining of C17.2 cells after 8 DIV following FACS with β III tubulin (*red*) and the nuclear stain TO-PRO-3 (*blue*). GFP expression is shown in *green*. *Scale bars* 50 μm. **g** The β III tubulin-positive cells were quantified after 8 DIV in SVCT2-over-expressing and empty vector-transduced cultures, and the average percentage from the total cells was plotted. A significant increase in the number of β III tubulin-positive cells is observed in the SVCT2-positive cultures. The results represent the mean ± SD (*n* = 5 for each group of two independent experiments). The nonparametric statistical analysis was performed using the Mann-Whitney posttest. *P < 0.05. **h–l** Cell death analysis measuring propidium iodide (PI) incorporation by flow cytometry after 8 DIV. **h, i**

The two-dimensional plots of the forward scatter (FSC) versus the side scatter (SSC) show the gate selection for further analysis in C17.2 cells transduced with pLB-GFP (**h**) or pLB-SVCT2-GFP (**i**). **j, k** The two-dimensional plots of the PE channel versus the FITC channel show the different populations of cells positive or negative for PI incorporation and GFP expression, respectively. **l** The total PI-positive cells (dead cells) from each culture were quantified, and the average percentage from the total cells was plotted. The number of dead cells doubled in SVCT2-positive cultures. The results represent the mean ± SD (*n* = 8) for each group of two independent experiments. The nonparametric statistical analysis was performed using the Mann-Whitney posttest. *P < 0.05

results showed that cultures over-expressing SVCT2 exhibited a higher number of cells positive for the neuronal marker (26.5 ± 5%) when compared with control cultures only expressing GFP (17.4 ± 4.8%); however, no enhanced neuronal morphology was observed in cells over-expressing SVCT2

(Fig. 8b, e, g). We also noted that the GFP fluorescence in SVCT2-over-expressing cultures seemed to be lost during the culture period, and that in the cells that remained SVCT2 positive, there was no clear correlation with β III tubulin expression (Fig. 8f). Because the loss of GFP fluorescence in

transduced C17.2 cells, which have stably integrated the gene of interest into their genome, could be due to cell death [22, 23], we performed a flow cytometry analysis of PI incorporation to evaluate changes in cell death. The PI fluorescence was measured in the PE channel, whereas the GFP fluorescence was monitored in the FITC channel. After 8 DIV, cultures transduced to over-express SVCT2 had a greater number of cells that had incorporated PI (11.3 ± 6.2% for GFP; 21.1 ± 5.6% for SVCT2) (Fig. 8j, k; $Q_1 + Q_2$ *population*, *L*). Furthermore, in both cultures, most PI-positive cells were GFP negative (Fig. 8j, k; Q_1 *population*). However, a considerable percentage of cells in both cultures were PI and GFP negative (Fig. 8j, k; Q_4 *population*), indicating that only part of the loss in GFP fluorescence was related to cell death.

Discussion

SVCT2 expression has been detected in the brains of adult rats and mice in several studies, showing a wide distribution; however, its presence has been mainly associated with the neuronal compartment, in which it is believed that it plays a protective role against oxidative stress [1, 4]. Previous studies have shown that the global expression of SVCT2 in cerebellar tissue increases during postnatal development [19], reaching the highest levels at adulthood. However, the dynamic pattern of SVCT2 expression during cerebellar postnatal development, a crucial moment at which differentiation is completed, was unexplored until now.

In the present study, we detected SVCT2 expression in postnatal cerebella isolated from newborn to fully grown adult mice. Our results show that after birth, SVCT2 expression is concentrated exclusively in the EGL, which harbors proliferative granular precursor cells. At intermediate stages of postnatal development, at which point granular precursor commitment to a neuronal fate increases, SVCT2 is heterogeneously detected in the EGL, suggesting the regulation of SVCT2 expression during differentiation. Higher SVCT2 expression was also observed in the transition zone between the EGL and IGL that most likely corresponded to the immature Purkinje cell plate, which is positive for the neuronal marker β III tubulin. This association between SVCT2 and β III tubulin was strongly exhibited in mature Purkinje neurons at P15 and P90, where high levels of the transporter were detected in cell bodies and primary branches. The presence of SVCT2 on the dendritic tree correlates with an earlier report showing that AA supplementation stimulates the expression of genes associated with synapse formation and plasticity, such as synaptotagmin 7, rabphilin 3A, and neurotrophic tyrosine kinase receptor [24], suggesting that high levels of SVCT2 in Purkinje neurons might be necessary to promote maturation and changes in plasticity. The only exception to the β III tubulin-SVCT2 association at the more adult stages was the detection of some

scattered cells in the white matter tracks that do not express the neuronal marker at P15. Under physiological conditions, it has been demonstrated that astrocytes do not express SVCT2; therefore, these cells could be undifferentiated. Interestingly, recent reports suggest the presence of a small population of neural stem cells within postnatal cerebellar tissues [25, 26].

In this study, we also detected SVCT2 expression in cerebellar neurospheres derived from murine P4 cerebella and in the cerebellar neural stem cell line C17.2, finding a tight correlation between SVCT2 and nestin expression. This correlates with our observation of SVCT2 expression in cerebellar granular progenitors and validates the notion that undifferentiated nestin-positive cells express the AA transporter, a concept established by our lab group in the adult neurogenic niche of the subventricular zone [17] and the cortical radial glia during embryonic development [18]. The use of the C17.2 cell line allowed us to characterize AA uptake through SVCT2, demonstrating that SVCT2 is functional in these cells, although it seems that it is largely accumulated in the intracellular compartment. This intracellular localization of SVCT2 has been previously reported in immortalized cell types [12, 27] and could be explained in terms of transporter recycling to and from the membrane to regulate AA uptake according to the needs of the cell [27].

Several studies have shown that AA promotes or enhances the differentiation of progenitor cells (e.g., embryonic stem [ES] cells, induced pluripotent stem cells [IPSCs], and tissue-specific ES cells) into different cell types, such as cardiocytes, osteoblasts, macrophages, and keratinocytes [28–34]. The search for neuronal differentiation factors has also led to the discovery that AA increases the expression of neurogenesis- and neuronal maturation-associated genes, enhancing the appearance of the neuronal phenotype in stem cell cultures [7, 8, 17, 24, 35–37]. In the present study, AA treatment of the cerebellar cell line C17.2 provides additional evidence for the role of AA in neuron generation and highlights the importance of SVCT2 in these precursor cells. A defined signaling pathway associated with the AA effect on neuronal differentiation has not been identified thus far; however, some studies in other cell types have shown that AA activates the PKC [31] and MAPK/ERK pathways [31, 38, 39]. Whether these same mechanisms are operating in AA-induced neural differentiation remains unanswered. In addition, recent evidence highlights an epigenetic role for AA in regulating gene expression during cellular reprogramming for the induction of pluripotent stem cells [40] and during the differentiation of dopaminergic neurons [9], through the activation of ten-eleven translocation (TET) dioxygenases, which catalyze the first step of active DNA demethylation, and the histone demethylases Jhdm1a/1b and JmjC [41]. For instance, it has been shown that AA treatment of embryonic fibroblasts induces H3K36me2/3 demethylation mediated by the demethylases Jhdm1a/1b [40], whereas AA treatment of embryonic midbrain NSCs induces

Tet1 and Jmjd3 activity, catalyzing the loss of cytosine methylation and the loss of H3K27m3 in the promoter regions of neuron-specific dopamine genes, allowing transcription factors access to these regions and therefore enhancing the differentiation of NSCs toward dopaminergic neurons [9]. After stably increasing SVCT2 expression levels in C17.2 cells, we observed a higher number of cells positive for β III tubulin expression, similar to when non-transduced cells were treated with AA. However, no neuronal-like morphological changes were detected, and no clear co-localization between SVCT2 and β III tubulin was seen. The loss of GFP fluorescence was also observed in the cultures after 8 DIV, which would indicate the loss of SVCT2 expression. Although our data show that the GFP expression was lost in part due to cell death, it has also been demonstrated that strong promoters, such as the cytomegalovirus (CMV) promoter present in our lentiviral vector system, are hypermethylated in cell culture and in transgenic animals [42–44], silencing the expression of the gene of interest. An analysis of PI incorporation revealed that SVCT2 over-expression increased the total number of dead cells by twofold. Because these cultures were not treated with AA, we can assume that the cell death was not because of the previously reported pro-apoptotic effects of AA at high concentrations [45, 46] but because of higher SVCT2 levels alone, through a still-undefined signaling route. Our C17.2 cell line characterization, in which spontaneous β III tubulin expression was detected over time, along with SVCT2 expression by these cells as well as P1 and P5 cerebellar sections led us to propose that undifferentiated neural precursors are positive for SVCT2, but that at intermediate stages of differentiation when neuronal commitment begins, β III tubulin expression rises while SVCT2 expression is low. Increasing levels of SVCT2 during this intermediate stage can induce cell death, suggesting that its expression and function must be finely tuned during neural stem cell differentiation. We know from the literature [17] and from our data on cerebellar tissue that SVCT2 is present in mature neurons; therefore, after neuronal commitment when differentiation is complete, there must be an increase in SVCT2 levels, so that maturation can proceed.

Further studies using Gulo$^{-/-}$ mice, an animal model that lacks the enzyme that synthesizes AA so AA levels can be regulated by dietary changes, in combination with NSC fate-mapping strategies and cell-specific SVCT2 loss/gain-of-function analyses might help unravel the role of AA in NSC differentiation toward a neuronal phenotype.

Conflict of interest The authors declare that they have no conflict of interest.

References

1. Harrison FE, May JM (2009) Vitamin C function in the brain: vital role of the ascorbate transporter SVCT2. Free Radic Biol Med 46(6):719–730
2. Nualart F, Salazar K, Oyarce K, Cisternas P, Jara N, Silva-Alvarez C, Pastor P, Martinez F et al (2012) Typical and atypical stem cells in the brain, vitamin C effect and neuropathology. Biol Res 45(3): 243–256
3. Oyarce K, Bongarzone ER, Nualart F (2014) Unconventional neurogenic niches and neurogenesis modulation by vitamins. Journal of Stem Cell Research & Therapy 4:184
4. Rice ME (2000) Ascorbate regulation and its neuroprotective role in the brain. Trends Neurosci 23(5):209–216
5. Kratzing CC, Kelly JD, Oelrichs BA (1982) Ascorbic acid in neural tissues. J Neurochem 39(3):625–627
6. Schaus R (1957) The ascorbic acid content of human pituitary, cerebral cortex, heart, and skeletal muscle and its relation to age. Am J Clin Nutr 5(1):39–41
7. Lee JY, Chang MY, Park CH, Kim HY, Kim JH, Son H, Lee YS, Lee SH (2003) Ascorbate-induced differentiation of embryonic cortical precursors into neurons and astrocytes. J Neurosci Res 73(2):156–165
8. Yan J, Studer L, McKay RD (2001) Ascorbic acid increases the yield of dopaminergic neurons derived from basic fibroblast growth factor expanded mesencephalic precursors. J Neurochem 76(1): 307–311
9. He XB, Kim M, Kim SY, Yi SH, Rhee YH, Kim T, Lee EH, Park CH et al (2015) Vitamin C facilitates dopamine neuron differentiation in fetal midbrain through TET1- and JMJD3-dependent epigenetic control manner. Stem Cells 33(4):1320–1332
10. Tsukaguchi H, Tokui T, Mackenzie B, Berger UV, Chen XZ, Wang Y, Brubaker RF, Hediger MA (1999) A family of mammalian Na$^+$-dependent L-ascorbic acid transporters. Nature 399(6731):70–75
11. Ulloa V, Garcia-Robles M, Martinez F, Salazar K, Reinicke K, Perez F, Godoy DF, Godoy AS et al (2013) Human choroid plexus papilloma cells efficiently transport glucose and vitamin C. J Neurochem 127(3):403–414
12. Caprile T, Salazar K, Astuya A, Cisternas P, Silva-Alvarez C, Montecinos H, Millan C, de Los Angeles Garcia M et al (2009) The Na$^+$-dependent L-ascorbic acid transporter SVCT2 expressed in brainstem cells, neurons, and neuroblastoma cells is inhibited by flavonoids. J Neurochem 108(3):563–577
13. Castro M, Caprile T, Astuya A, Millan C, Reinicke K, Vera JC, Vasquez O, Aguayo LG et al (2001) High-affinity sodium-vitamin C co-transporters (SVCT) expression in embryonic mouse neurons. J Neurochem 78(4):815–823
14. Qiu S, Li L, Weeber EJ, May JM (2007) Ascorbate transport by primary cultured neurons and its role in neuronal function and protection against excitotoxicity. J Neurosci Res 85(5):1046–1056
15. Gess B, Lohmann C, Halfter H, Young P (2010) Sodium-dependent vitamin C transporter 2 (SVCT2) is necessary for the uptake of L-ascorbic acid into Schwann cells. Glia 58(3):287–299
16. Garcia M, Salazar K, Millan C, Rodriguez F, Montecinos H, Caprile T, Silva C, Cortes C et al (2005) Sodium vitamin C cotransporter SVCT2 is expressed in hypothalamic glial cells. Glia 50(1):32–47
17. Pastor P, Cisternas P, Salazar K, Silva-Alvarez C, Oyarce K, Jara N, Espinoza F, Martinez AD et al (2013) SVCT2 vitamin C transporter expression in progenitor cells of the postnatal neurogenic niche. Front Cell Neurosci 7:119
18. Silva-Alvarez C, Salazar K, Cisternas P, Martinez F, Liour S, Jara N, Bertinat R, Nualart F (2016) Apical polarization of SVCT2 in apical radial glial cells and progenitors during brain development. Mol Neurobiol. (in press)

19. Meredith ME, Harrison FE, May JM (2011) Differential regulation of the ascorbic acid transporter SVCT2 during development and in response to ascorbic acid depletion. Biochem Biophys Res Commun 414(4):737–742

20. Salazar K, Martinez M, Ulloa V, Bertinat R, Martinez F, Jara N, Espinoza F, Bongarzone ER, Nualart F (2016) SVCT2 overexpression in neuroblastoma cells induces cellular branching that is associated with ERK signaling. Mol Neurobiol 53(10):6668–6679

21. Snyder EY, Deitcher DL, Walsh C, Arnold-Aldea S, Hartwieg EA, Cepko CL (1992) Multipotent neural cell lines can engraft and participate in development of mouse cerebellum. Cell 68(1):33–51

22. Manjunath N, Shankar P, Stockton B, Dubey PD, Lieberman J, von Andrian UH (1999) A transgenic mouse model to analyze CD8(+) effector T cell differentiation in vivo. Proc Natl Acad Sci U S A 96(24):13932–13937

23. Strebel A, Harr T, Bachmann F, Wernli M, Erb P (2001) Green fluorescent protein as a novel tool to measure apoptosis and necrosis. Cytometry 43(2):126–133

24. Shin DM, Ahn JI, Lee KH, Lee YS, Lee YS (2004) Ascorbic acid responsive genes during neuronal differentiation of embryonic stem cells. Neuroreport 15(12):1959–1963

25. Klein C, Butt SJ, Machold RP, Johnson JE, Fishell G (2005) Cerebellum- and forebrain-derived stem cells possess intrinsic regional character. Development 132(20):4497–4508

26. Lee A, Kessler JD, Read TA, Kaiser C, Corbeil D, Huttner WB, Johnson JE, Wechsler-Reya RJ (2005) Isolation of neural stem cells from the postnatal cerebellum. Nat Neurosci 8(6):723–729

27. Acuna AI, Esparza M, Kramm C, Beltran FA, Parra AV, Cepeda C, Toro CA, Vidal RL et al (2013) A failure in energy metabolism and antioxidant uptake precede symptoms of Huntington's disease in mice. Nat Commun 4:2917

28. Cao N, Liu Z, Chen Z, Wang J, Chen T, Zhao X, Ma Y, Qin L et al (2012) Ascorbic acid enhances the cardiac differentiation of induced pluripotent stem cells through promoting the proliferation of cardiac progenitor cells. Cell Res 22(1):219–236

29. Pasonen-Seppanen S, Suhonen TM, Kirjavainen M, Suihko E, Urtti A, Miettinen M, Hyttinen M, Tammi M et al (2001) Vitamin C enhances differentiation of a continuous keratinocyte cell line (REK) into epidermis with normal stratum corneum ultrastructure and functional permeability barrier. Histochem Cell Biol 116(4):287–297

30. Qiao H, May JM (2009) Macrophage differentiation increases expression of the ascorbate transporter (SVCT2). Free Radic Biol Med 46(8):1221–1232

31. Savini I, Catani MV, Rossi A, Duranti G, Melino G, Avigliano L (2002) Characterization of keratinocyte differentiation induced by ascorbic acid: protein kinase C involvement and vitamin C homeostasis. The Journal of investigative dermatology 118(2):372–379

32. Takahashi T, Lord B, Schulze PC, Fryer RM, Sarang SS, Gullans SR, Lee RT (2003) Ascorbic acid enhances differentiation of embryonic stem cells into cardiac myocytes. Circulation 107(14):1912–1916

33. Takamizawa S, Maehata Y, Imai K, Senoo H, Sato S, Hata R (2004) Effects of ascorbic acid and ascorbic acid 2-phosphate, a long-acting vitamin C derivative, on the proliferation and differentiation of human osteoblast-like cells. Cell Biol Int 28(4):255–265

34. Wu X, Zeng LH, Taniguchi T, Xie QM (2007) Activation of PKA and phosphorylation of sodium-dependent vitamin C transporter 2 by prostaglandin E2 promote osteoblast-like differentiation in MC3T3-E1 cells. Cell Death Differ 14(10):1792–1801

35. Haramoto M, Tatemoto H, Muto N (2008) Essential role of ascorbic acid in neural differentiation and development: high levels of ascorbic acid 2-glucoside effectively enhance nerve growth factor-induced neurite formation and elongation in PC12 cells. J Health Sci 54(1):43–49

36. Lau T, Adam S, Schloss P (2006) Rapid and efficient differentiation of dopaminergic neurons from mouse embryonic stem cells. Neuroreport 17(10):975–979

37. Yu DH, Lee KH, Lee JY, Kim S, Shin DM, Kim JH, Lee YS, Lee YS et al (2004) Changes of gene expression profiles during neuronal differentiation of central nervous system precursors treated with ascorbic acid. J Neurosci Res 78(1):29–37

38. Bowie AG, O'Neill LA (2000) Vitamin C inhibits NF-kappa B activation by TNF via the activation of p38 mitogen-activated protein kinase. J Immunol 165(12):7180–7188

39. Lee SA, Son YO, Kook SH, Choi KC, Lee JC (2011) Ascorbic acid increases the activity and synthesis of tyrosinase in B16F10 cells through activation of p38 mitogen-activated protein kinase. Arch Dermatol Res 303(9):669–678

40. Wang T, Chen K, Zeng X, Yang J, Wu Y, Shi X, Qin B, Zeng L et al (2011) The histone demethylases Jhdm1a/1b enhance somatic cell reprogramming in a vitamin-C-dependent manner. Cell Stem Cell 9(6):575–587

41. Young JI, Zuchner S, Wang G (2015) Regulation of the epigenome by vitamin C. Annu Rev Nutr 35:545–564

42. Prosch S, Stein J, Staak K, Liebenthal C, Volk HD, Kruger DH (1996) Inactivation of the very strong HCMV immediate early promoter by DNA CpG methylation in vitro. Biol Chem Hoppe Seyler 377(3):195–201

43. Kong Q, Wu M, Huan Y, Zhang L, Liu H, Bou G, Luo Y, Mu Y et al (2009) Transgene expression is associated with copy number and cytomegalovirus promoter methylation in transgenic pigs. PLoS One 4(8):e6679

44. Mehta AK, Majumdar SS, Alam P, Gulati N, Brahmachari V (2009) Epigenetic regulation of cytomegalovirus major immediate-early promoter activity in transgenic mice. Gene 428(1–2):20–24

45. Leung PY, Miyashita K, Young M, Tsao CS (1993) Cytotoxic effect of ascorbate and its derivatives on cultured malignant and nonmalignant cell lines. Anticancer Res 13(2):475–480

46. Paolini M, Pozzetti L, Pedulli GF, Marchesi E, Cantelli-Forti G (1999) The nature of prooxidant activity of vitamin C. Life Sci 64(23):PL 273–PL 278